2013

Structure and thermodynamics of H3O+(H2O)8 clusters: A combined molecular dynamics and quantum mechanics approach

Berhane Temelso
berhane.temelso@furman.edu

Thorsten Koddermann
SCAI, tkoeddermann@scai.fraunhofer.de

Karl K. Kirschner
SCAI, kkirsch@scai.fraunhofer.de

Katurah L. Klein
Bucknell University, klk02@mcsdk12.org

George C. Shields
Bucknell University, gcs012@bucknell.edu

Computational and Theoretical Chemistry 1021 (2013) 240–248

Contents lists available at ScienceDirect

Computational and Theoretical Chemistry

journal homepage: www.elsevier.com/locate/comptc

Structure and thermodynamics of $H_3O^+(H_2O)_8$ clusters: A combined molecular dynamics and quantum mechanics approach

Berhane Temelso [a], Thorsten Köddermann [b,c], Karl N. Kirschner [b,c,*], Katurah Klein [a], George C. Shields [a,*]

[a] Dean's Office, College of Arts and Sciences, and Department of Chemistry, Bucknell University, Lewisburg, PA 17837, United States
[b] Department of Virtual Material Design, Fraunhofer-Institute for Algorithms and Scientific Computing (SCAI), 53754 Sankt Augustin, Germany
[c] Department of Bioinformatics, Fraunhofer-Institute for Algorithms and Scientific Computing (SCAI), 53754 Sankt Augustin, Germany

ARTICLE INFO

Article history:
Received 19 May 2013
Received in revised form 25 July 2013
Accepted 25 July 2013
Available online 6 August 2013

Keywords:
Hydronium
MP2
Molecular dynamics
Force field optimization
Solvation of protons
Hydrogen bonding

ABSTRACT

We have studied the structure and stability of $H_3O^+(H_2O)_8$ clusters using a combination of molecular dynamics sampling and high-level *ab initio* calculations. 20 distinct oxygen frameworks are found within 2 kcal/mol of the electronic or standard Gibbs free energy minimum. The impact of quantum zero-point vibrational corrections on the relative stability of these isomers is quite significant. The box-like isomers are favored in terms of electronic energy, but with the inclusion of zero-point vibrational corrections and entropic effects tree-like isomers are favored at higher temperatures. Under conditions from 0 to 298.15 K, the global minimum is predicted to be a tree-like structure with one dangling singly coordinated water molecule. Above 298.15 K, higher entropy tree-like isomers with two or more singly coordinated water molecules are favored. These assignments are generally consistent with experimental IR spectra of $(H_3O^+)(H_2O)_8$ obtained at ~150 K.

1. Introduction

Water is an extremely important molecule that, as far as we know, uniquely exists in abundance on Earth. The Earth's water cycle is a complex interplay of solid, liquid and gaseous states of water, and this cycle is involved in many different chemical, thermodynamic, and environmental events [1]. While our understanding of the water cycle has improved because of interest in global warming and space exploration, our atomistic understanding of water clusters and aerosols is not complete [2,3]. Here, we present a computational investigation of how eight water molecules interact with a hydronium ion in the gas phase. The hydronium ion and its hydration is an inherent part of aqueous solutions, gas-phase clusters, and aerosols. Improving our understanding of the configuration and thermodynamics of $H_3O^+(H_2O)_8$, or $H^+(H_2O)_9$, clusters is an important step in elucidating how water molecules form larger clusters and, subsequently, aerosols in the atmosphere. This work is a continuation of long-standing efforts to explore ion–molecule interactions [4–8], hydrogen-bonded interactions [9–11,16–28], water cluster formation [3,4,9–20], and atmospheric processes [5–8,12,21–28].

Theoreticians have investigated water–hydronium clusters since at least 1970 [29,30]. Many groups have used quantum mechanics (QM) calculations to optimize structures and energies of $H_3O^+(H_2O)_n$ with $n = 1–21$ [4,29–60]. Most of these calculations have been on species of particular interest, such as $H_3O^+(H_2O)$ (Zundel cation) and $H_3O^+(H_2O)_{20}$ (a magic number of stable water molecules), with fewer on medium sized clusters ranging in size from $H_3O^+(H_2O)_4$ to $H_3O^+(H_2O)_{10}$ [4,35,37,39,41,43,48,49,51,54,56].

Once the nonbonded cluster reaches a certain size (i.e. more than ~5 molecules), sampling configurational space becomes increasingly difficult. To address this, several research groups have used Monte Carlo, molecular dynamics (MD), and basin hopping techniques to sample and generate different configurations [46–48,54,61–67]. Karthikeyan and Kim [48] performed the highest level calculations on $H_3O^+(H_2O)_8$; they employed the Resolution-of-the-identity (RI) second-order Møller–Plesset perturbation theory (MP2) [68] method, extrapolated to the complete basis set limit, and corrected for higher-order correlation using CCSD(T). They identified 9 possible cluster configurations within 4.3 kcal/mol of their identified elctronic energy (E_e) global minimum. A recent study by Bankura and Chandra identified 6 low energy clusters using counterpoise corrected MP2/6-31+G* electronic energies [54]. Unfortunately the clusters' coordinates from these two research efforts are not available as Supplementary information, making their direct comparison difficult. Herein, we improve on

* Corresponding authors. Department of Bioinformatics, Fraunhofer- Institute for Algorithms and Scientific Computing (SCAI), 53754 Sankt Augustin, Germany (K.N. Kirschner), Dean's Office, College of Arts and Sciences, and Department of Chemistry, Bucknell University, Lewisburg, PA 17837, United States Tel.: +1 570 577 3292 (G.C. Shields).

E-mail addresses: kkirsch@scai.fraunhofer.de (K.N. Kirschner), george.shields@bucknell.edu (G.C. Shields).

2210-271X/$ - see front matter © 2013 Elsevier B.V. All rights reserved.
http://dx.doi.org/10.1016/j.comptc.2013.07.039

this previous work by (a) generating a large number of isomers via an MD simulation that employs a newly optimized H_3O^+ force field and integrate isomers from existing literature, (b) filtering these isomers using a series of RI-MP2 *ab initio* calculations, (c) employing a more robust basis set extrapolation scheme, and (d) eliminating unreliable CCSD(T) corrections that use small basis sets [69,70]. Our extensive sampling of structures from an MD simulation, combined with previously reported unique structures [62,71], result in 51 low energy conformers that fall into 20 unique groups as defined by their oxygen skeleton framework. The effect that zero-point vibrational energy (ZPVE), entropy, and temperature have on the relative stability of the isomers is discussed.

2. Computational methods

Classical molecular dynamics simulations of $H_3O^+(H_2O)_{1-6}$ clusters in vacuum, an H_3O^+ ion in liquid water, and several H_3O^+ ions in a saturated water/HCl solution were carried out in the isobaric–isothermal (NPT) ensemble in order to parameterize an all atom force field for the H_3O^+ ion. With the newly parameterized hydronium force field, a production run of a $H_3O^+(H_2O)_8$ cluster was performed in order to generate cluster structures that sample the conformational space of the $H_3O^+(H_2O)_8$ system.

The force field used is represented by a sum of pair-wise additive interatomic Lennard–Jones (LJ) and Coulombic potentials:

$$U = \sum_{i=1}^{N-1}\sum_{j>1}^{N}[U^{LJ}(r_{ij}) + U^{Coul}(r_{ij})] \tag{1}$$

with

$$U^{LJ} = 4\varepsilon_{ij}\left[\left(\frac{\sigma_{ij}}{r_{ij}}\right)^{12} - \left(\frac{\sigma_{ij}}{r_{ij}}\right)^{6}\right] \tag{2}$$

$$U^{Coul} = \frac{q_i q_j}{4\pi\varepsilon_0 r_{ij}} \tag{3}$$

All intramolecular bonds and angles of the molecules and ions were kept fixed. Electrostatic interactions were computed using the particle mesh Ewald summation method with a real space cutoff of 1.2 nm, a mesh spacing of approximately 0.12 nm, and fourth order interpolations [72]. The OPLS combining rules were applied. Temperature and pressure control was achieved using a Nosé–Hoover thermostat and the Rahman–Parrinello barostat with coupling times $\tau_T = 0.5$ ps and $\tau_p = 2.0$ ps. Equilibrium runs took 1 ns and were followed by 10 ns trajectories with 2 fs time steps. The TIP4P-Ew model [73] was used to model H_2O, while the force field published by Joung and Cheatham [74] was used to model Cl^- since it was explicitly parameterized for use with TIP4P-Ew. All simulations were carried out using the Gromacs-4.0.5 package [75].

The purpose of the current force-field development is to parameterize an all-atom force field for H_3O^+ that can reproduce experimental macro- and microscopic properties. The structure of H_3O^+ was optimized at the MP2/6-31+G* theory level using the GAMESS package [76]. All bonds and angles are kept fixed, and there is no possibility of proton transfer. The total charge of the hydronium was enforced to be +1, enabling it to be used in very different environments, from vacuum to the condensed phase. Since the resulting H_3O^+ force field should be compatible with the molecular mechanics water model, we used TIP4-EW's LJ parameters and partial atomic charges as our initial values. In the parameterization process the first condensed-phase simulation contained 585 H_2O and 1 H_3O^+, while the second contained 585 H_2O, 60 H_3O^+, and 60 Cl^- to model a saturated water/HCl solution. All condensed-phase simulations were performed under periodic boundary conditions at 1 bar and 300 K. The vacuum simulations of the $H_3O^+(H_2O)_{1-6}$ clusters were performed at 150 K without periodic boundary conditions and with translational and rotational degrees of freedom switched off.

The partial charges, the position of the virtual site, and the LJ-parameters shown in Table 1 were iteratively changed to reproduce (a) the previously computed and experimental enthalpy of solvation ($\Delta H^{exp.} = -115.0$ and $\Delta H^{sim.} = -116.7$ [77,78]), (b) the standard formation enthalpies of water/hydronium clusters in vacuum (Fig. 1), and (c) H^{H3O+}---O^{H2O} and H^{H3O+}---H^{H2O} radial distribution functions (RDFs) of a saturated HCl solution (Fig. 2). The standard solvation enthalpy was obtained from the intermolecular potential energy of the dissolved hydronium at 298 K; it was assumed that the vapor phase is formed by isolated hydronium ions, making it unnecessary to simulate the ion in the vacuum. In all three comparisons, the MD simulations using the optimized force field perform well. As seen in Fig. 1, representing the solution-phase behavior, the position of the peaks overlap well with experimental position [79], and the area-under-the-curves are also in relatively close agreement. Likewise, the stepwise addition of 1–6 water molecules reproduces experimental gas-phase enthalpies well [80]. The optimized H_3O^+ force-field parameters are given in Table 1.

The same simulation parameters were used in the production run of the $H_3O^+(H_2O)_8$ cluster as used in the vacuum simulations of the $H_3O^+(H_2O)_{1-6}$ systems. This simulation was run for 10 ns at a temperature of 150.0 K. Exactly 200 snapshots of the atomic coordinates were produced, one every 50 ps, and used as input into the QM structure optimization. RI-MP2, as implemented in ORCA 2.9 [81], was used to obtain fully optimized structures and energies. To this list of MD-identified structures, we added 42 low energy clusters found by Hodges and Wales [62] using their anisotropic site potential (ASP) potential [39]. These minima were determined by first performing three basin hopping runs of 30,000 quenches using the simple Kozack-Jordan (KJ) [82] potential and reoptimizing the low energy structures using the more elaborate ASP potential. Those coordinates are deposited in the Cambridge Cluster Database [71].

RI-MP2 uses density fitting to expand four-index two electron integrals in terms of two- and three-index two electron integrals that are cheaper to compute and transform [83]. As a result, it is less expensive than conventional MP2 while maintaining the same level of accuracy, particularly for modeling hydrogen bonded systems [84]. When applied in conjunction with correlation consistent basis sets that can be extrapolated to their complete basis set (CBS) limit, such as the aug-cc-pVNZ (abbreviated as aVNZ, where N = D, T, Q, ...) [85,86], it yields benchmark quality binding energies, equilibrium geometries and vibrational frequencies. The MD structures were first minimized using RI-MP2/6-31G*, resulting in better refined structures at a reasonable cost [34,17]. The RI-MP2/6-31G* optimized structures were then subject to RI-MP2/aVDZ single-point energy calculations, and all isomers whose relative energy was more than 6 kcal/mol higher than the lowest energy isomer were excluded. The remaining unique low energy

Table 1
Force field parameters for the hydronium ion parameterized in this work.

Atom type	σ (nm)	ε (kJ/mol)	q (e)
OH	0.0	0.0	−2.78
HH	0.11	0.5	1.26
MH	0.3843	0.6810	0.0
Geometry	r (nm)	φ (°)	
OH-HH	0.9686		
OH-MH	0.0500		
HH-OH-HH		113.0	
HH-OH-MH		107.0	

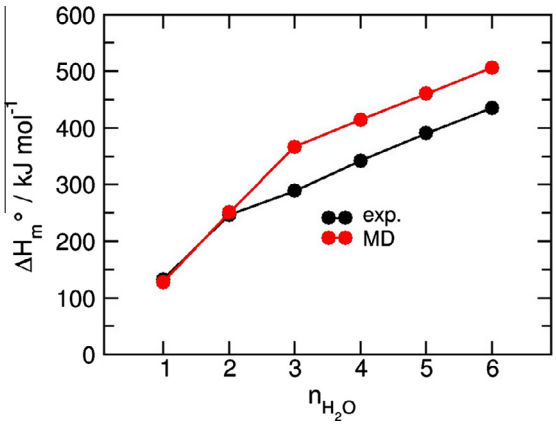

Fig. 1. The MD simulated and experimental [80] intermolecular molar standard formation enthalpies of water/hydronium clusters in vacuum as a function of 1–6 water molecules.

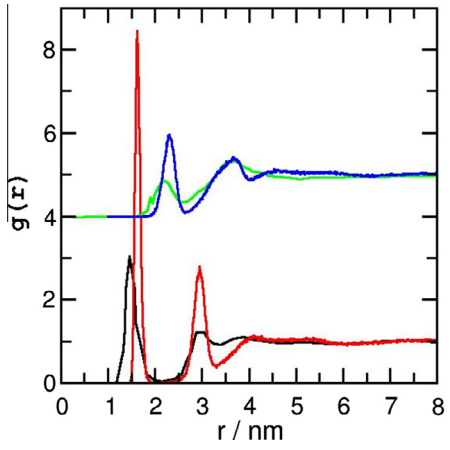

Fig. 2. The MD simulated and experimental radial distribution functions of a saturated HCl solution. The experimental [79] RDFs are measured between a hydronium hydrogen and a water oxygen (Exp: black line; MD: red) or water hydrogen (Exp: green; MD: blue; offset for clarity). (For interpretation of the references to color in this figure legend, the reader is referred to the web version of this article.) Reproduced from Ref. [66] with permission of the PCCP Owner Societies.

isomers were optimized using RI-MP2/aVDZ with tight convergence criteria on the SCF wavefunction, energies, gradients and displacements. The harmonic vibrational frequencies, needed to calculate the ZPVE and finite temperature thermodynamic corrections to the enthalpy (H) and entropy (S), were also determined using RI-MP2/aVDZ. Furthermore, the RI-MP2 CBS limit energies were calculated using a basis set extrapolation scheme. This 4–5 inverse polynomial extrapolation [87] has been used extensively for water clusters:

$$E_{\mathrm{CBS}}^{\mathrm{RI\text{-}MP2}} = E_{\mathrm{N}}^{\mathrm{RI\text{-}MP2}} + \frac{b}{(N+1)^4} + \frac{c}{(N+1)^5} \tag{4}$$

where $E_{\mathrm{N}}^{\mathrm{RI\text{-}MP2}}$ is an RI-MP2/aVNZ//aVDZ energy, $E_{\mathrm{CBS}}^{\mathrm{RI\text{-}MP2}}$ is the extrapolated RI-MP2/CBS energy, N is the largest angular momentum number for the aVNZ basis set (N = 2, 3, 4 for N = D, T, Q, respectively), and b and c are fitting parameters. Least-squares fitting of the RI-MP2/aVNZ//aVDZ (N = D, T, Q) binding energies to Eq. (4) yields the RI-MP2/CBS energy for a given cluster (see Table 2).

The most stable structure at a given temperature is determined by combining the RI-MP2/CBS electronic energy with finite temperature thermodynamic corrections assuming ideal gas conditions with a rigid-rotor approximation for molecular rotations and a harmonic oscillator model for vibrations. The harmonic vibrational frequencies were not scaled since uniform scaling factors do not change the relative stability of the isomers notably. The binding energy (ΔE_i) of isomer i was calculated as the energy difference between the cluster and infinitely separated constituents:

$$\Delta E_i = E[H_3O^+(H_2O)_8]_i - E[H_3O^+] - 8 * E[H_2O] \tag{5}$$

The relative energy ($\Delta\Delta E_i$) of cluster i was calculated using the global minimum as a reference:

$$\Delta\Delta E_i = E[H_3O^+(H_2O)_8]_i - \mathrm{MIN}_{n=1\ldots N}\{E[H_3O^+(H_2O)_8]_n\} \tag{6}$$

The binding [ΔG(T)] and relative [$\Delta\Delta G$(T)] Gibbs free energies were calculated similarly. Standard state conditions are 1 atm pressure and the stated temperature. All molecular graphics are generated with Chimera 1.7 using its default hydrogen bond definition [88].

3. Results and discussion

3.1. MD simulation and configurational sampling

MD simulations are a useful tool for sampling the $H_3O^+(H_2O)_8$ configurational space in vacuum. Since the intermolecular interactions are realistic, every snapshot extracted from the simulation trajectory represents a thermodynamically meaningful structure and can be directly used as input for an *ab initio* structure optimization. An overlay of the structures extracted from MD simulations with the eventual *ab initio* optimized minima shows good agreement, particularly for the more stable species, as shown in Fig. S1.

The experimental enthalpy of formation data (Fig. 1) suggests that the addition of a third water molecule to the $H_3O^+(H_2O)_2$ cluster has a significant influence on the average hydrogen bond energy. Since this is a quantum effect, it is very difficult to reproduce using classical mechanics. Thus, the force field was optimized to provide all hydrogen bonds the same energetic value such that the solvation enthalpy, the radial distribution function in the HCl solution, and the hydrogen bond strength of the first two water molecules in the gas phase are optimally reproduced. The linearity of the simulated data at n = 3 with the first two data points is because the third hydrogen bond has the same strength as the first two hydrogen bonds in the classical model. The slope of the curve after n = 3 mirrors the experimental slope [80] because the subsequent water molecules do not form hydrogen bonds with the hydronium, instead binding to another water molecule. It is unavoidable to have this curve offset if we wish to reasonably model the bulk phase since the experimental hydrogen bond average may change in going from the gas to the bulk phase.

The vast diversity of hydrogen bonding topologies available for $H_3O^+(H_2O)_8$ necessitates reliable configurational sampling. In our case, MD simulations at 150 K provided 200 structures that yielded the Gibbs free energy minima for $T \geqslant 0$ K. However, optimizations starting with the 42 ASP minima [62] largely yielded structures that had low electronic energy, but high Gibbs free energies at most finite temperatures. Therefore, it was necessary to combine the ASP and MD starting structures to sample all important hydrogen bonding motifs over the entire temperature range of interest.

3.2. Structures and stability

Of the 242 initial structures, 51 unique isomers have electronic energy within 6 kcal/mol of the RI-MP2/CBS electronic energy global minimum. Thirty-six of these 51 have relative electronic energy ($\Delta\Delta E_e$), zero-point corrected energy ($\Delta\Delta E_0$) or standard Gibbs free

Table 2
RI-MP2/CBS[a] binding energies for the lowest energy members of the 20 isomer groups of $H_3O^+(H_2O)_8$.[b]

#HBs	Isomer	CBS	0 K	150 K		298.15 K	
		ΔE_e	ΔH	ΔH	ΔG	ΔH	ΔG
13	A	−**144.93**	−123.27	−**129.70**	−91.45	−**130.87**	−52.94
12	B	−144.06	−122.96	−129.19	−91.55	−130.16	−53.73
12	C	−143.44	−122.66	−128.83	−91.33	−129.78	−53.64
11	D	−143.15	−123.13	−129.02	−92.53	−129.76	−55.94
12	E	−143.10	−122.28	−128.43	−90.99	−129.33	−53.39
11	F	−143.08	−**123.31**	−128.98	−**92.84**	−129.56	−56.67
12	G	−142.98	−122.65	−128.60	−91.79	−129.37	−54.88
12	H	−142.83	−122.45	−128.39	−91.55	−129.15	−54.60
13	I	−142.76	−121.51	−127.72	−90.10	−128.65	−52.30
11	J	−142.73	−122.67	−128.55	−91.93	−129.13	−55.27
13	K	−142.58	−121.44	−127.64	−89.97	−128.51	−52.14
12	L	−142.27	−122.25	−128.06	−91.56	−128.66	−55.03
12	M	−142.05	−121.73	−127.70	−90.64	−128.32	−53.53
11	N	−142.05	−122.54	−128.18	−92.16	−128.72	−56.12
12	O	−141.98	−121.51	−127.59	−90.35	−128.34	−53.01
12	P	−141.98	−121.39	−127.34	−90.50	−128.07	−53.57
11	Q	−141.41	−121.65	−127.34	−91.42	−127.86	−55.48
11	R	−141.29	−122.18	−127.65	−91.98	−128.02	−56.36
11	S	−141.21	−122.23	−127.64	−92.14	−127.98	−**56.72**
11	T	−140.73	−121.33	−126.96	−91.05	−127.45	−55.14

[a] RI-MP2/aVDZ//aVDZ, RI-MP2/aVTZ//aVDZ, RI-MP2/aVQZ//aVDZ binding energies extrapolated using Eq. (4).
[b] All energies are in kcal/mol. Global minima shown in bold.

energy ($\Delta\Delta G^0$) that are within 2 kcal/mol of the absolute minima for $\Delta\Delta E_e$, $\Delta\Delta E_0$, or $\Delta\Delta G^0$. These 36 low energy isomers can be further categorized into 20 different groups based on their oxygen skeleton and hydrogen bond topology; we report the lowest energy isomer of each group in Fig. 3 in order of increasing electronic energy.

The hydrated proton is in an Eigen form (H_3O^+) in all the clusters with the O–H bond distance of the H_3O^+ moiety spanning a range of 0.99–1.05 Å. with an average of 1.022 Å. There is no indication of a shared proton – the nearest oxygen of a water molecule to the H_3O^+ hydrogens is at least 1.45 Å away. The H_3O^+ donates three strong HBs to the surrounding water molecules as previously seen in experimental infrared spectra [66,89–91], and low energy structures for $H_3O^+(H_2O)_n$ where $n \geqslant 3$ [49,54–56,62]. The H_3O^+--H_2O HBs are strong as evidenced by their average distance of 1.54 Å versus 1.86 Å for H_2O--H_2O HBs. Such large geometric differences are understandable considering that the electronic binding energy H_3O^+–H_2O is about 34 kcal/mol

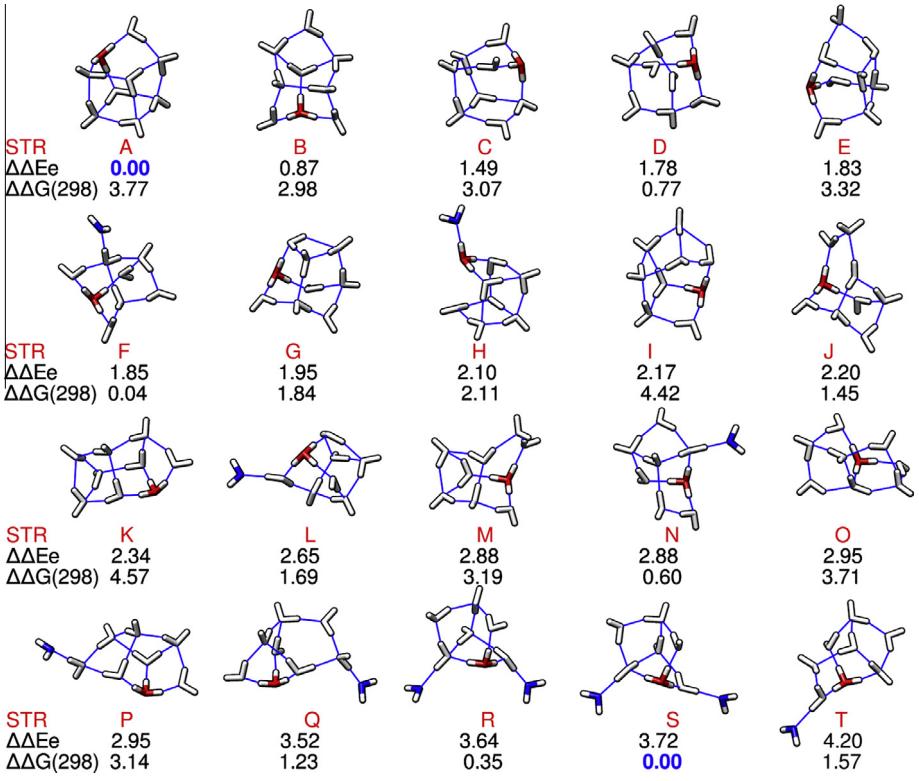

Fig. 3. RI-MP2/CBS//aVDZ low energy isomers of $H_3O^+(H_2O)_8$ ordered by increasing relative electronic energy, $\Delta\Delta E_e$. $\Delta\Delta G(298)$ represents the relative free energy at a standard state of 298.15 K and 1 atm. The hydronium ion is shown in red and the dangling water in white for visibility; the other waters appear gray. (For interpretation of the references to color in this figure legend, the reader is referred to the web version of this article.)

compared to just 5 kcal/mol for H_2O–H_2O [45]. The hydronium oxygen does not accept a hydrogen bond because of hydrogen–hydrogen repulsion. As a result, H_3O^+ remains on the surface in all reported structures. Only when $n \geqslant 17$ do clathrate cage structures with either a water molecule or hydronium ion encapsulated become competitive with the surface H_3O^+ [54,62,64]. However, because of the nature of the MD input structure (i.e. covalent bonds between all hydrogen and heavy atoms) it is possible that the *ab initio* optimization performed at 0 K never had a chance to sample the proton in a Zundel form due to a proton transfer barrier. Experimental and computational studies have suggested that larger clusters can adopt Zundel forms [42,50,55,58,90,92]. While interesting, an investigation of Eigen versus Zundel forms of the cation within the identified $H_3O^+(H_2O)_8$ clusters is beyond the scope of this work.

The most stable isomers in terms of RI-MP2/CBS electronic energy are the box-like structures with every water molecule doubly (DA, DD, AA) or triply (DAA, DDA) coordinated, where "D" indicates a hydrogen bond donor and "A" an acceptor. Such is the case, for example, with structures A–E. At higher energies, tree-like isomers become more prominent with one or two singly coordinated water molecules that dangle as a hydrogen bond acceptor ("A"). These motifs are favored in terms of free energies with increasing temperature due to their higher entropic content. This interplay between the enthalpic stabilization and the entropic penalty for forming hydrogen bonds (HBs) is responsible for the competition between the box-like and tree-like structures. Even though the presence of more HBs generally correlates with higher stability in terms of electronic energy, it does not fully explain the observations here. For example, in Table 3 some isomers that have 13 HBs are less stable than others with 11 HBs. This is mainly because of the large variation in the strength of the hydrogen bonds involved.

As illustrated in Fig. 4, the 20 isomers fall within a ~4 kcal/mol range, in terms of electronic energy, and only one isomer is within 1 kcal/mol of the global minimum structure A. However, the inclusion of ZPVE decreases the relative energy separation between the 20 isomers to about 2 kcal/mol. the global minimum structure also changes from isomer A to isomer F. Adding finite temperature corrections increases the relative energy spectrum at higher temperatures because of entropic effects. Since isomers A, F, and S are

Table 3
RI-MP2/CBS[a] relative energies of the lowest energy members of the 20 isomer groups of $H_3O^+(H_2O)_8$.[b]

#HBs	Isomer	CBS	0 K	150 K		298.15 K	
		$\Delta\Delta E_e$	$\Delta\Delta H$	$\Delta\Delta H$	$\Delta\Delta G$	$\Delta\Delta H$	$\Delta\Delta G$
13	A	**0.00**	0.04	**0.00**	1.39	**0.00**	3.77
12	B	0.87	0.35	0.51	1.29	0.71	2.98
12	C	1.49	0.65	0.87	1.52	1.09	3.07
11	D	1.78	0.18	0.68	0.31	1.11	0.77
12	E	1.83	1.02	1.26	1.85	1.54	3.32
11	F	1.85	**0.00**	0.72	**0.00**	1.31	0.04
12	G	1.95	0.65	1.10	1.05	1.50	1.84
12	H	2.10	0.86	1.31	1.29	1.72	2.11
13	I	2.17	1.80	1.98	2.74	2.22	4.42
11	J	2.20	0.63	1.15	0.91	1.74	1.45
13	K	2.34	1.87	2.06	2.88	2.35	4.57
12	L	2.65	1.05	1.64	1.28	2.21	1.69
12	M	2.88	1.58	2.00	2.20	2.55	3.19
11	N	2.88	0.76	1.51	0.68	2.15	0.60
12	O	2.95	1.80	2.11	2.49	2.52	3.71
12	P	2.95	1.92	2.35	2.34	2.79	3.14
11	Q	3.52	1.65	2.36	1.42	3.00	1.23
11	R	3.64	1.12	2.05	0.86	2.85	0.35
11	S	3.72	1.08	2.06	0.70	2.89	**0.00**
11	T	4.20	1.98	2.74	1.79	3.42	1.57

[a] RI-MP2/aVDZ//aVDZ, RI-MP2/aVTZ//aVDZ, RI-MP2/aVQZ//aVDZ binding energies extrapolated using Eq. (4).
[b] All energies are in kcal/mol. Global minima shown in bold.

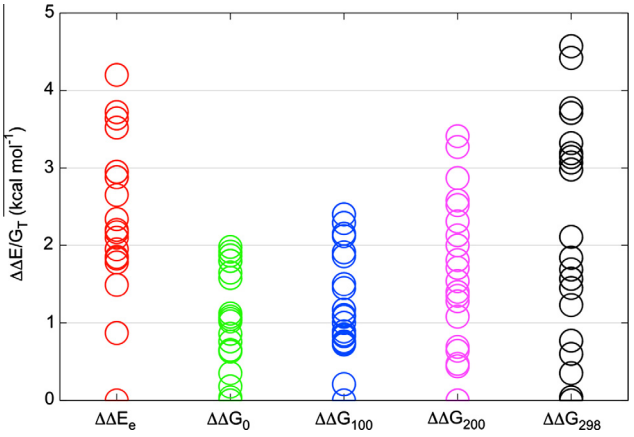

Fig. 4. The RI-MP2/CBS relative electronic ($\Delta\Delta E_e$) and free ($\Delta\Delta G_T$) energies of the 20 isomers at various temperatures. Inclusion of the ZPVE makes box-like and tree-like structures more competitive, leading to a higher density of isomers at 0 K. Entropic corrections increase the free energy differences with temperature.

representative of the most important structural motifs, we examined the change in their relative free energies as a function of temperature at 1 atm pressure in Fig. 5. It is clear that isomer F (and possibly others with a single dangling water molecule) have the most stable structures for $T < 290$ K. For $T > 290$ K, isomer S and presumably others with two or more dangling water molecules are most likely to be observed.

There are substantial differences between the structures of pure water clusters, $(H_2O)_n$ [17,18], and hydrated protons $(H^+)(H_2O)_n$. While small water clusters form cyclic minima for $n < 6$ and quasi-planar or three-dimensional structures for $n \geqslant 6$, hydrated protons adopt very different configurations. For $(H^+)(H_2O)_n$, branched or chain-like structures are dominant for $n < \sim 10$ and two-dimensional net structures are common for $\sim 10 < n < 21$, while three-dimensional cages are favored for $n \geqslant 21$ [89,91]. This behavior strongly suggests that the proton or hydronium ion profoundly perturbs the structure of water clusters in the gas phase. In the case of $H_3O^+(H_2O)_8$, the box-like isomer A has the same oxygen framework as the lowest energy $(H_2O)_9$ isomers – both have stacked water tetramers and pentamers. However, the $(H_2O)_9$ structures have homodromic hydrogen bonding networks that are largely absent in the box-like isomers of $H_3O^+(H_2O)_8$. A comparison of $H_3O^+(H_2O)_8$ with $NH_4^+(H_2O)_8$ reveals significant spectral and structural similarities such as the presence of surface cations and box-like structures with one or two singly coordinated water molecules [7,93].

Nuclear quantum effects such as zero-point motion and tunneling affect strength of hydrogen bonds, and the relative population and interconversion between different isomers at any finite temperature [94–96]. While accounting for these effects is theoretically difficult and computationally expensive, there has been a lot of progress running path integral molecular dynamics (PIMD) [97,98] on full dimensional *ab initio* potentials to capture them [67]. Due to the impact that ZPVE corrections have on the relative stability of the clusters, future calculations that attempt to better account for anharmonicity (e.g. using *ab initio*-based diffusion Monte Carlo) [99] would be intriguing. Anharmonic corrections have been shown to be important at reproducing experimental vibrational frequencies under 1000 cm^{-1} in the water dimer [16]. Recent *ab initio*-based simulations performed on neutral water clusters have shown that nuclear quantum effects can alter the relative stability of isomers at temperatures below 150 K [67]. Considering the quantum nature of the extra proton present in the charged clusters presented here, accounting for these effects could have a notable effect on their relative stability. While the role of

quantum effects on these clusters remains an open question, their electronic binding energy has been determined using high level *ab initio* methods.

3.3. Comparison to previous calculations

Karthikeyan and Kim [48], whose computational investigation is the most similar to ours, employed Halkier's [100,101] two-point inverse cubic extrapolation scheme using aVDZ–aVTZ and aVTZ–aVQZ basis sets to obtain RI-MP2/CBS energies. Since the convergence of the binding energy with increasing basis sets is not monotonic, a two-point extrapolation with an inverse cubic function can lead to erroneous CBS limits. Our investigations of basis set extrapolation schemes for hydrogen-bonded systems [18,27], all demonstrate that Halkier's extrapolation using the aVNZ (N = D, T, Q) basis sets gives lower RI-MP2 binding energies than benchmark values. Conversely, the 4–5 inverse polynomial scheme [Eq. (4)] we employ here matches benchmark values very closely. This polynomial also converges the counterpoise corrected and uncorrected binding energies to the same limit, whereas employing the Halkier extrapolation leads to slightly different limits. Bryantsev and coworkers [45] also tested many extrapolation schemes for $(H_2O)_n$, $(OH^-)(H_2O)_n$, and $(H_3O^+)(H_2O)_n$, concluding that the 4–5 inverse polynomial scheme provides the most reliable binding energy.

Unlike Karthikeyan and Kim [48], we did not include higher-order electron correlation corrections with a small basis set,

$$\delta_{\mathrm{MP2}}^{\mathrm{CCSD(T)}} = E[\mathrm{CCSD(T)/aVDZ//MP2/aVDZ}] - E[\mathrm{MP2/aVDZ}] \qquad (7)$$

because such corrections using a small double-zeta basis set (e.g. aVDZ) are unreliable. Recent work from the Sherrill and Tschumper groups discovered a significant discrepancy when including CCSD(T) corrections with a small basis set for a series of non-covalently bonded systems [69,70]. Therefore, MP2/CBS energies are likely more reliable than CCSD(T)/CBS estimates, if the $\delta_{\mathrm{MP2}}^{\mathrm{CCSD(T)}}$ correction is not calculated using a triple-zeta or larger basis.

3.4. Comparison with experimental IR spectra

Many experimental groups have used infrared (IR) spectroscopy to probe OH stretching and bending regions of size selected $(H^+)(H_2O)_n$ clusters in an effort to derive structural information. Miyazaki and coworkers [89] looked at the OH stretching for n = 4–27 and concluded that chain-like structures are dominant for $n < \sim 10$, two-dimensional net structures are common for $\sim 10 < n < 21$, and three-dimensional cages are favored for $n \geqslant 21$. Similar work by Shin and coworkers [90] deduced the presence of a "magic number" cluster at n = 21, based on the evolution of a dangling OH group excitation as a function of cluster size. Headrick and coworkers [91] observed unique bands in the bending and stretching region of $(H^+)(H_2O)_{n=2-11}$, and confirmed the presence of structures with one or two dangling water molecules for n = 2–11. In all of these experiments, the temperature of the clusters is not clearly defined, making comparisons between calculated and experimentally inferred results difficult. In Lin and coworkers' vibrational predissociation spectroscopic experiments on $(H^+)(H_2O)_{n=9-11}$, the cluster temperatures were estimated to be around 150 K [66]. Their spectra in the 2700–3900 cm^{-1} region showed small peaks at ~3740 and ~3650 cm^{-1} that correspond to the asymmetric and symmetric free OH stretch of a singly-coordinated dangling (A) water molecule for $n \leqslant 9$. These peaks essentially disappear by n = 11. The implications of their work for $(H^+)(H_2O)_9$ is that clusters with at least one dangling water molecule are indeed present, and that other clusters may be thermally populated (Fig. 5).

Fig. 6 shows a comparison between the experimental[66] and RI-MP2/aVDZ calculated IR spectrum of isomers A, F, and S in the 3600–3800 cm^{-1} region. We scaled the harmonic frequencies by 0.9604 [102] to allow for a more direct spectrum comparison and fitted each spectral line (red) to a Gaussian function (blue) with a 15 cm^{-1} full-width at half-maximum height (FWHM). The scaling factor should correct the expected blue shift of the harmonic vibrational spectra relative to the experimental and anharmonic analogs [56], particularly for the H_3O^+ stretching modes in the 2000 cm^{-1} region. The signature peaks at ~3650 and ~3740 cm^{-1} are indicative of a dangling water molecule, such as present in isomers F and S.

As shown in Fig. 6, Isomer F appears to best match the experimental spectrum. As mentioned above, other isomers might also contribute to the spectrum, and their concentrations will be temperature dependent. From our set of isomers, five have relative free energies that are within 1 kcal/mol of the global minimum F at 150 K. These include isomers D (+0.31), N (+0.68), S (+0.70), R (+0.86) and J (+0.91). Of these, isomers N, S, and R are likely candidates since they have either one or two dangling water molecules. Furthermore, the second lowest isomer of motif group F, (see F1 in Fig. S1, Supplementary Materials) lies 0.1–0.2 kcal/mol higher than isomer F. Considering that 150 K is equivalent to 0.30 kcal/mol of thermal energy, we believe that F and F1 are the biggest contributors to the observed spectrum. Aside from the presence of many nearly degenerate isomers at any finite temperature, interconversion between these isomers through thermodynamic and kinetic processes makes assigning an experimental spectrum to a particular isomer challenging.

Anharmoncity corrections to the vibrational spectra of hydrogen-bonded systems are significant because of the inherent limits of a harmonic potential and the coupling of vibrational modes [103]. Torrent-Sucarrat and Anglada investigated the effect of anharmonicity on the vibrational spectra of $H^+(H_2O)_3$, $H^+(H_2O)_4$, and $H^+(H_2O)_{21}$ using second-order vibrational perturbation theory (VPT2) [104] on B3LYP potential energy surfaces [56]. They concluded that anharmonic corrections are essential to match experimental spectra with harmonic vibrational spectral lines, particularly for the H_3O^+ stretching modes in the 2000 cm^{-1} region. Chaban et al. reached similar conclusions on the basis of their anharmonic calculations using a vibrational self-consistent field (VSCF) [105] method and its correlation corrected analog (CC-VSCF) on a MP2 potential energy surface for $H^+(H_2O)$ and $H^+(H_2O)_2$ [40]. Despite the importance of anharmonicity, applying simple scaling factors to harmonic frequencies to match experimental spectral lines is still very effective for high frequency

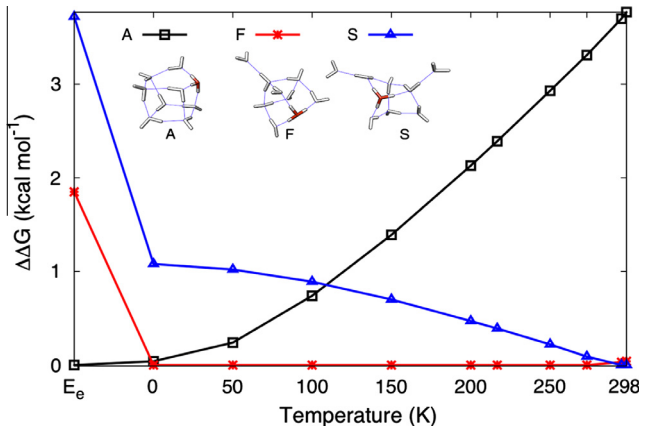

Fig. 5. The RI-MP2/CBS relative stability of the three dominant motifs of $H_3O^+(H_2O)_8$ as a function of temperature.

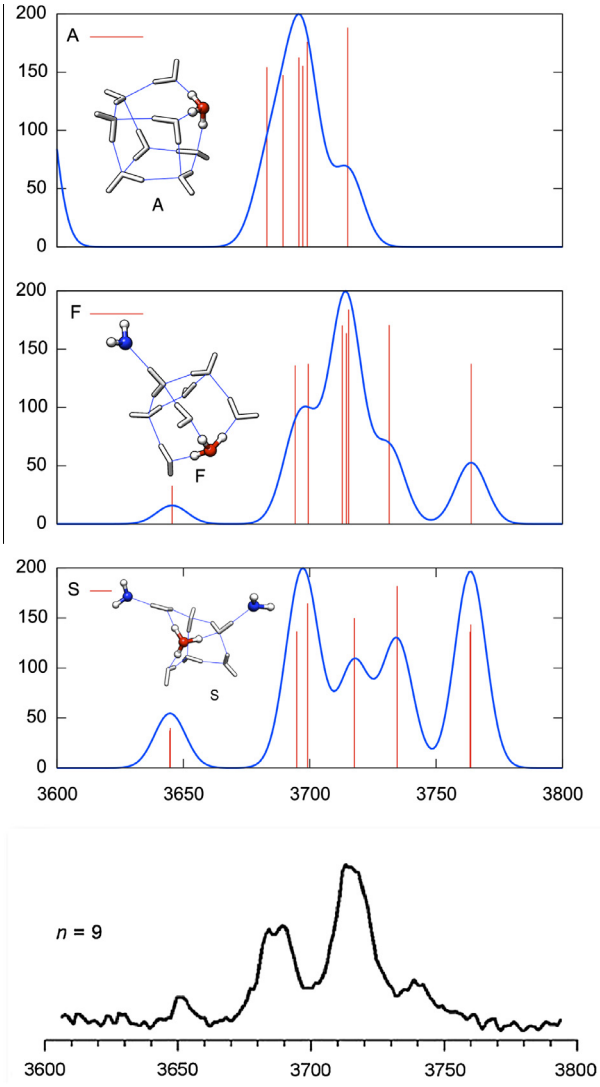

Fig. 6. The experimental [66] (bottom) and RI-MP2/aVDZ calculated (top) IR spectrum of isomers A, F, and S in the 3600–3800 cm^{-1} region. The calculated frequencies are scaled by 0.9604 and each spectral line (red) is fitted to a Gaussian function (blue) with a 15 cm^{-1} full-width at half-maximum height (FWHM). The symmetric and asymmetric OH stretch peaks at ~3650 and ~3740 cm^{-1} are indicative of a dangling water like that present in isomers F and S. Isomer F matches the experimental spectrum best. Reproduced from Ref. [66] with permission of the PCCP Owner Societies. (For interpretation of the references to color in this figure legend, the reader is referred to the web version of this article.)

(larger than 3000 cm^{-1}) vibrational modes like the OH stretching modes used here to assign signatures. Therefore, assigning specific isomers to experimental spectra based on these high frequency OH stretching modes should be meaningful even though the presence and interconversion of isomers cannot be ruled out.

4. Conclusions

We have studied the structure and thermodynamics of $(H_3O^+)(H_2O)_8$ using molecular dynamics sampling and high-level *ab initio* calculations. We find 20 distinct groups, based on their oxygen framework, within 2 kcal/mol of the electronic or standard Gibbs free energy. The impact of quantum ZPVE corrections on the relative stability of these isomers is quite significant, thereby presenting a challenge for classical force fields. The box-like isomers are favored in terms of electronic energy, but including ZPVE corrections and entropic effects result in tree-like isomers as the global minima at higher temperatures. Under conditions from 0 K to room temperature, the global minimum is a tree-like structure with one dangling singly coordinated (A) water molecule. Above 290 K, tree-like isomers with two or more singly coordinated water molecules are the global minima. These assignments are generally consistent with experimental IR spectra of $(H_3O^+)(H_2O)_8$ at ~150 K; structures with one or two dangling water molecules are responsible for the experimentally observed vibrational spectra.

Acknowledgements

Acknowledgment is made to the NSF, Bucknell University, and the Fraunhofer-Institute for Algorithms and Scientific Computing (SCAI) for their support of this work. This project was supported in part by NSF Grant CHE-0848827, CHE-1213521, and by NSF Grants CHE-0116435, CHE-0521063, CHE-0849677, and CHE-1229354 as part of the MERCURY high-performance computer consortium (http://www.mercuryconsortium.org).

Appendix A. Supplementary material

Supplementary data associated with this article can be found, in the online version, at http://dx.doi.org/10.1016/j.comptc.2013.07.039.

References

[1] M.R. Allen, W.J. Ingram, Constraints on future changes in climate and the hydrologic cycle, Nature 419 (2002) 224–232.
[2] R. Ludwig, Water: from clusters to the bulk, Angew. Chem. Int. Ed. 40 (2001) 1808–1827.
[3] C. Pérez et al., Structures of cage, prism, and book isomers of water hexamer from broadband rotational spectroscopy, Science 336 (2012) 897–901.
[4] M.W. Jurema, K.N. Kirschner, G.C. Shields, Modeling of magic water clusters $(H_2O)_{20}$ and $(H_2O)_{21}H^+$ with the PM3 quantum-mechanical method, J. Comput. Chem. 14 (1993) 1326–1332.
[5] F.C. Pickard, M.E. Dunn, G.C. Shields, Comparison of model chemistry and density functional theory thermochemical predictions with experiment for formation of ionic clusters of the ammonium cation complexed with water and ammonia; Atmospheric implications, J. Phys. Chem. A 109 (2005) 4905–4910.
[6] F.C. Pickard et al., Comparison of CBS-QB3, CBS-APNO, G2, and G3 thermochemical predictions with experiment for formation of ionic clusters of hydronium and hydroxide ions complexed with water, J. Chem. Phys. 122 (2005) 024302.
[7] T.E. Morrell, G.C. Shields, Atmospheric implications for formation of clusters of ammonium and 1–10 water molecules, J. Phys. Chem. A 114 (2010) 4266–4271.
[8] D.E. Husar et al., Hydration of the bisulfate ion: atmospheric implications, J. Phys. Chem. A 116 (2012) 5151–5163.
[9] M.W. Jurema, G.C. Shields, Ability of the PM3 quantum mechanical method to model *inter*molecular hydrogen bonding between neutral molecules, J. Comput. Chem. 14 (1993) 89–104.
[10] K.N. Kirschner, G.C. Shields, Quantum-Mechanical Investigation of Large Water Clusters, Int. J. Quantum Chem. (1994) 349–360.
[11] G.C. Shields, K.N. Kirschner, The limitations of certain density functionals in modeling neutral water clusters, Synth. React. Inorg. Met. – Org. Chem. 38 (2008) 32–36.
[12] M.E. Dunn, E.K. Pokon, G.C. Shields, Thermodynamics of forming water clusters at various temperatures and pressures by Gaussian-2, Gaussian-3, complete basis set-QB3, and complete basis set-APNO model chemistries; implications for atmospheric chemistry, J. Am. Chem. Soc. 126 (2004) 2647–2653.
[13] M.E. Dunn, E.K. Pokon, G.C. Shields, The ability of the Gaussian-2, Gaussian-3, complete basis set-QB3, and complete basis set-APNO model chemistries to model the geometries of small water clusters, Int. J. Quantum Chem. 100 (2004) 1065–1070.
[14] M.B. Day, K.N. Kirschner, G.C. Shields, Pople's Gaussian-3 model chemistry applied to an investigation of $(H_2O)_8$ water clusters, Int. J. Quantum Chem. 102 (2005) 565–572.
[15] M.B. Day, K.N. Kirschner, G.C. Shields, Global search for minimum energy $(H_2O)_{21}H^+$ clusters, $n = 3–5$, J. Phys. Chem. A 109 (2005) 6773–6778.
[16] M.E. Dunn et al., Prediction of accurate anharmonic experimental vibrational frequencies for water clusters, $(H_2O)_n$, $n = 2–5$, J. Phys. Chem. A 110 (2006) 303–309.
[17] R.M. Shields et al., Accurate predictions of water cluster formation, $(H_2O)_{n=2-10}$, J. Phys. Chem. A 114 (2010) 11725–11737.

[18] B. Temelso, K.A. Archer, G.C. Shields, Benchmark structures and binding energies of small water clusters with anharmonicity corrections, J. Phys. Chem. A 115 (2011) 12034–12046.
[19] B. Temelso, G.C. Shields, The role of anharmonicity in hydrogen-bonded systems: the case of water clusters, J. Chem. Theory Comput. 7 (2011) 2804–2817.
[20] C. Pérez et al., Broadband Fourier transform rotational spectroscopy for structure determination: the water heptamer, Chem. Phys. Lett. 571 (2013) 1–15.
[21] M.A. Allodi et al., Do hydroxyl radical-water clusters, $OH(H_2O)_n$, $n = 1–5$, exist in the atmosphere?, J Phys. Chem. A 110 (2006) 13283–13289.
[22] K.S. Alongi et al., Exploration of the potential energy surfaces, prediction of atmospheric concentrations, and prediction of vibrational spectra for the $HO_2 \cdots (H_2O)_n$ ($n = 1–2$) hydrogen bonded complexes, J. Phys. Chem. A 110 (2006) 3686–3691.
[23] K.N. Kirschner et al., In search of $CS_2(H_2O)(n = 1–4)$ clusters, J. Chem. Phys. 126 (2007) 154320.
[24] M.A. Allodi, K.N. Kirschner, G.C. Shields, Thermodynamics of the hydroxyl radical addition to isoprene, J. Phys. Chem. A 112 (2008) 7064–7071.
[25] M.E. Dunn et al., Experimental and theoretical study of the OH vibrational spectra and overtone chemistry of gas-phase vinylacetic acid, J. Phys. Chem. A 112 (2008) 10226–10235.
[26] G.M. Hartt, G.C. Shields, K.N. Kirschner, Hydration of OCS with one to four water molecules in atmospheric and laboratory conditions, J. Phys. Chem. A 112 (2008) 4490–4495.
[27] B. Temelso et al., Quantum mechanical study of sulfuric acid hydration: atmospheric implications, J. Phys. Chem. A 116 (2012) 2209–2224.
[28] B. Temelso, T.N. Phan, G.C. Shields, Computational study of the hydration of sulfuric acid dimers: implications for acid dissociation and aerosol formation, J. Phys. Chem. A 116 (2012) 9745–9758.
[29] P.A. Kollman, L.C. Allen, Theory of the strong hydrogen bond. Ab initio calculations on HF_2^- and $H_5O_2^+$[1a], J. Am. Chem. Soc. 92 (1970) 6101–6107.
[30] W.P. Kraemer, G.H.F. Diercksen, SCF MO LCGO studies on hydrogen bonding: the system $(H_2OHOH_2)^+$, Chem. Phys. Lett. 5 (1970) 463–465.
[31] M.D. Newton, S. Ehrenson, Ab initio studies on the structures and energetics of inner- and outer-shell hydrates of the proton and the hydroxide ion, J. Am. Chem. Soc. 93 (1971) 4971–4990.
[32] L.L. Ingraham, The mechanism of proton transfers, Biochim. Biophys. Acta (BBA) – Gen. Sub. 279 (1972) 8–14.
[33] W. Meyer, W. Jakubetz, P. Schuster, Correlation effects on energy curves for proton transfer. The cation $[H_5O_2]^+$, Chem. Phys. Lett. 21 (1973) 97–102.
[34] M.D. Newton, Ab initio studies of the hydrated H_3O^+ ion. II. The energetics of proton motion in higher hydrates ($n = 3–5$), J. Chem. Phys. 67 (1977) 5535–5546.
[35] S. Scheiner, Proton transfers in hydrogen-bonded systems. Cationic oligomers of water, J. Am. Chem. Soc. 103 (1981) 315–320.
[36] S. Yamabe, T. Minato, K. Hirao, Ab initio calculation of the thermochemical data on the $H_3O + H_2O = H_5O_2^+$ gas-phase clustering, J. Chem. Phys. 80 (1984) 1576–1578.
[37] J.Y. Choi, E.R. Davidson, I. Lee, AM1 studies on the potential energy surface for the proton transfer in protonated water clusters, $H^+(H_2O)_n$, J. Comput. Chem. 10 (1989) 163–175.
[38] K. Laasonen, M.L. Klein, Structural study of $(H_2O)_{20}$ and $(H_2O)_{21}H^+$ using density functional methods, J. Phys. Chem. 98 (1994) 10079–10083.
[39] M.P. Hodges, A.J. Stone, Modeling small hydronium–water clusters, J. Chem. Phys. 110 (1999) 6766–6772.
[40] G.M. Chaban, J.O. Jung, R.B. Gerber, Anharmonic vibrational spectroscopy of hydrogen-bonded systems directly computed from ab initio potential surfaces: $(H_2O)_n$, $n = 2, 3$; $Cl^-(H_2O)_n$, $n = 1, 2$; $H^+(H_2O)_n$, $n = 1, 2$; $H_2O–CH_3OH$, J. Phys. Chem. A 104 (2000) 2772–2779.
[41] A. Khan, Ab initio studies of $(H_2O)_{20}H^+$ and $(H_2O)_{21}H^+$ prismic, fused cubic and dodecahedral clusters: can H_3O^+ ion remain in cage cavity?, Chem Phys. Lett. 319 (2000) 440–450.
[42] J.-C. Jiang et al., Infrared spectra of $H^+(H_2O)_{5–8}$ clusters: evidence for symmetric proton hydration, J. Am. Chem. Soc. 122 (2000) 1398–1410.
[43] T. James, D.J. Wales, Protonated water clusters described by an empirical valence bond potential, J. Chem. Phys. 122 (2005).
[44] M. Jieli, T. Miyake, M. Aida, Enumeration of topology-distinct structures and possible stable structures of protonated water clusters, $H_3O^+(H_2O)_{n-1}$ ($n \leqslant 5$), Bull. Chem. Soc. Jpn. 80 (2007) 2131–2136.
[45] V.S. Bryantsev et al., Evaluation of B3LYP, X3LYP, and M06-class density functionals for predicting the binding energies of neutral, protonated, and deprotonated water clusters, J. Chem. Theory Comput. 5 (2009) 1016–1026.
[46] S. Karthikeyan et al., Structure, stability, thermodynamic properties, and infrared spectra of the protonated water octamer $H^+(H_2O)_8$, J. Phys. Chem. A 112 (2008) 10120–10124.
[47] S. Karthikeyan, K.S. Kim, Structure, stability, thermodynamic properties, and IR spectra of the protonated water decamer $H^+(H_2O)_{10}$, J. Phys. Chem. A 113 (2009) 9237–9242.
[48] S. Karthikeyan, K.S. Kim, Structure, stability, thermodynamic properties and IR spectra of the protonated water cluster $H^+(H_2O)_9$, Mol. Phys. 107 (2009) 1169–1176.
[49] T. Kus et al., An ab initio study of the $(H_2O)_{20}H^+$ and $(H_2O)_{21}H^+$ water clusters, J. Chem. Phys. 131 (2009) 104313.
[50] Y. Luo, S. Maeda, K. Ohno, Automated exploration of stable isomers of $H^+(H_2O)_n$ ($n = 5–7$) via ab initio calculations: an application of the anharmonic downward distortion following algorithm, J. Comput. Chem. 30 (2009) 952–961.
[51] Q.C. Nguyen, Y.-S. Ong, J.-L. Kuo, A hierarchical approach to study the thermal behavior of protonated water clusters $H^+(H_2O)_n$, J. Chem. Theory Comput. 5 (2009) 2629–2639.
[52] D.J. Anick, Topology-energy relationships and lowest energy configurations for pentagonal dodecahedral, $(H_2O)_{20}X$ clusters, X = empty, H_2O, NH_3, H_3O^+: the importance of O-topology, J. Chem. Phys. 132 (2010) 12.
[53] M. Kaledin, C.A. Wood, Ab initio studies of structural and vibrational properties of protonated water cluster $H_7O_3^+$ and its deuterium isotopologues: an application of driven molecular dynamics, J. Chem. Theory Comput. 6 (2010) 2525–2535.
[54] A. Bankura, A. Chandra, A first principles theoretical study of the hydration structure and dynamics of an excess proton in water clusters of varying size and temperature, Chem. Phys. 387 (2011) 92–102.
[55] P. Goyal, M. Elstner, Q. Cui, Application of the SCC-DFTB method to neutral and protonated water clusters and bulk water, J. Phys. Chem. B 115 (2011) 6790–6805.
[56] M. Torrent-Sucarrat, J.M. Anglada, Anharmonicity and the Eigen–Zundel dilemma in the IR spectrum of the protonated 21 water cluster, J. Chem. Theory Comput. 7 (2011) 467–472.
[57] H. Do, N.A. Besley, Structural optimization of molecular clusters with density functional theory combined with basin hopping, J. Chem. Phys. 137 (2012) 134106–134109.
[58] G. Meraj, M. Naganathappa, A. Chaudhari, Energetics during proton transfer process in hydrated zündel ion complex, Int. J. Quantum Chem. 112 (2012) 1439–1448.
[59] S. Nachimuthu, J. Gao, D.G. Truhlar, A benchmark test suite for proton transfer energies and its use to test electronic structure model chemistries, Chem. Phys. 400 (2012) 8–12.
[60] P. Parkkinen, S. Riikonen, L. Halonen, Global minima of protonated water clusters $(H_2O)_{20}H^+$ revisited, J. Phys. Chem. A 116 (2012) 10826–10835.
[61] E. Kochanski, Theoretical studies of the system $H_3O^+(H_2O)_n$ for $n = 1, 9$, J. Am. Chem. Soc. 107 (1985) 7869–7873.
[62] M.P. Hodges, D.J. Wales, Global minima of protonated water clusters, Chem. Phys. Lett. 324 (2000) 279–288.
[63] A.V. Egorov, E.N. Brodskaya, A. Laaksonen, Solid–liquid phase transition in small water clusters: a molecular dynamics simulation study, Mol. Phys. 100 (2002) 941–951.
[64] C. Wu et al., Protonated clathrate cages enclosing neutral water molecules: $H^+(H_2O)_{21}$ and $H^+(H_2O)_{28}$, J. Chem. Phys. 122 (2005) 074315.
[65] J.L. Kuo, M.L. Klein, Structure of protonated water clusters: low-energy structures and finite temperature behavior, J. Chem. Phys. 122 (2005).
[66] C.K. Lin et al., Vibrational predissociation spectra and hydrogen-bond topologies of $H^+(H_2O)_{9–11}$, Phys. Chem. Chem. Phys. 7 (2005) 938–944.
[67] Y. Wang et al., The water hexamer: cage, prism, or both. Full dimensional quantum simulations say both, J. Am. Chem. Soc. 134 (2012) 11116–11119.
[68] C. Møller, M.S. Plesset, Note on an approximation treatment for many-electron systems, Phys. Rev. 46 (1934) 618–622.
[69] M.S. Marshall, L.A. Burns, C.D. Sherrill, Basis set convergence of the coupled-cluster correction, ΔMP2-CCSD(T): best practices for benchmarking non-covalent interactions and the attendant revision of the S22, NBC10, HBC6, and HSG databases, J. Chem. Phys. 135 (2011) 194102.
[70] E.J. Carrell, C.M. Thorne, G.S. Tschumper, Basis set dependence of higher-order correlation effects in pi-type interactions, J. Chem. Phys. 136 (2012) 14103–14111.
[71] D.J. Wales, et al., The Cambridge Cluster, Database, 2013.
[72] U. Essmann et al., A smooth particle mesh Ewald method, J. Chem. Phys. 103 (1995) 8577–8593.
[73] H.W. Horn et al., Development of an improved four-site water model for biomolecular simulations: TIP4P-Ew, J. Chem. Phys. 120 (2004) 9665–9678.
[74] I.S. Joung, Cheatham, Determination of alkali and halide monovalent ion parameters for use in explicitly solvated biomolecular simulations, J. Phys. Chem. B 112 (2008) 9020–9041.
[75] B. Hess et al., GROMACS 4: algorithms for highly efficient, load-balanced, and scalable molecular simulation, J. Chem. Theory Comput. 4 (2008) 435–447.
[76] M.S. Gordon, M.W. Schmidt, Advances in electronic structure theory: GAMESS a decade later, in: M.S. Gordon, M.W. Schmidt, C.E. Dykstra (Eds.), Theory and Applications of Computational Chemistry: The First Forty Years, Elsevier, Amsterdam, Boston, 2005, pp. 1167–1189.
[77] J.-F. Gal, P.-C. Maria, E.D. Raczynska, Thermochemical aspects of proton transfer in the gas phase, J. Mass Spectrom. 36 (2001) 699–716.
[78] L.X. Dang, Solvation of the hydronium ion at the water liquid/vapor interface, J. Chem. Phys. 119 (2003) 6351–6353.
[79] A. Botti et al., Ions in water: the microscopic structure of a concentrated HCl solution, J. Chem. Phys. 121 (2004) 7840–7848.
[80] Y.K. Lau, S. Ikuta, P. Kebarle, Thermodynamics and kinetics of the gas-phase reactions: $H_3O^+(H_2O)_{n-1}$ + water = $H_3O^+(H_2O)_n$, J. Am. Chem. Soc. 104 (1982) 1462–1469.
[81] F. Neese, The ORCA program system, Wiley Interdiscipl. Rev.: Comput. Mol. Sci. 2 (2012) 73–78.
[82] R.E. Kozack, P.C. Jordan, Polarizability effects in a four-charge model for water, J. Chem. Phys. 96 (1992) 3120.

[83] M. Feyereisen, G. Fitzgerald, A. Komornicki, Use of approximate integrals in Ab initio theory, an application in MP2 energy calculations, Chem. Phys. Lett. 208 (1993) 359–363.
[84] M.S. Marshall et al., An error and efficiency analysis of approximations to Møller–Plesset perturbation theory, J. Chem. Theory Comput. 6 (2010) 3681–3687.
[85] T. Dunning, Gaussian-basis sets for use in correlated molecular calculations. 1. The atoms boron through neon and hydrogen, J. Chem. Phys. 90 (1989) 1007–1023.
[86] R. Kendall, T. Dunning, R. Harrison, Electron-affinities of the 1st-row atoms revisited, a systematic basis-sets and wave-functions, J. Chem. Phys. 96 (1992) 6796–6806.
[87] S.S. Xantheas, On the importance of the fragment relaxation energy terms in the estimation of the basis set superposition error correction to the intermolecular interaction energy, J. Chem. Phys. 104 (1996) 8821–8824.
[88] E.F. Pettersen et al., UCSF chimera – a visualization system for exploratory research and analysis, J. Comput. Chem. 25 (2004) 1605–1612.
[89] M. Miyazaki et al., Infrared spectroscopic evidence for protonated water clusters forming nanoscale cages, Science 304 (2004) 1134–1137.
[90] J.W. Shin et al., Infrared signature of structures associated with the $H^+(H_2O)_n$ (n = 6 to 27) clusters, Science 304 (2004) 1137–1140.
[91] J.M. Headrick et al., Spectral signatures of hydrated proton vibrations in water clusters, Science 308 (2005) 1765–1769.
[92] K. Mizuse, A. Fujii, Tuning of the internal energy and isomer distribution in small protonated water clusters $H^+(H_2O)_{4-8}$: an application of the inert gas messenger technique, J. Phys. Chem. A 116 (2012) 4868–4877.
[93] J. Douady, F. Calvo, F. Spiegelman, Structure, stability, and infrared spectroscopy of $(H_2O)[NH_4]^+$ clusters: a theoretical study at zero and finite temperature, J. Chem. Phys. 129 (2008) 154305–154314.
[94] M.E. Tuckerman, D. Marx, On the quantum nature of the shared proton in hydrogen bonds, Science 275 (1997) 817.
[95] D. Marx et al., The nature of the hydrated excess proton in water, Nature 397 (1999) 601–604.
[96] X.Z. Li, B. Walker, A. Michaelides, Quantum nature of the hydrogen bond, Proc. Nat. Acad. Sci. 108 (2011) 6369–6373.
[97] E.L. Pollock, D.M. Ceperley, Simulation of quantum many-body systems by path-integral methods, Phys. Rev. B 30 (1984) 2555–2568.
[98] M.E. Tuckerman et al., Efficient molecular dynamics and hybrid Monte Carlo algorithms for path integrals, J. Chem. Phys. 99 (1993) 2796–2808.
[99] B.L. Hammond, W.A. Lester, P.J. Reynolds, Monte Carlo Methods in Ab Initio Quantum Chemistry, World Scientific, Singapore, 1994.
[100] A. Halkier et al., Basis-set convergence in correlated calculations on Ne, N_2, and H_2O, Chem. Phys. Lett. 286 (1998) 243–252.
[101] A. Halkier et al., Basis-set convergence of the energy in molecular Hartree–Fock calculations, Chem. Phys. Lett. 302 (1999) 437–446.
[102] P. Sinha et al., Harmonic vibrational frequencies: scaling factors for HF, B3LYP, and MP2 methods in combination with correlation consistent basis sets, J. Phys. Chem. A 108 (2004) 9213–9217.
[103] S.S. Xantheas, Anharmonic vibrational spectra of hydrogen bonded clusters: comparison between higher energy derivative and mean-field grid based methods, Int. Rev. Phys. Chem. 25 (2006) 719–733.
[104] V. Barone, Vibrational zero-point energies and thermodynamic functions beyond the harmonic approximation, J. Chem. Phys. 120 (2004) 3059–3065.
[105] R.B. Gerber, M.A. Ratner, A semiclassical self-consistent field (SC SCF) approximation for eigenvalues of coupled-vibration systems, Chem. Phys. Lett. 68 (1979) 195–198.